PREPARED FOR THE U.S. DEPARTMENT OF ENERGY,
UNDER CONTRACT DE-AC02-76-CHO-3073

PPPL-2815
UC-420,426

PPPL-2815

THE EFFECT OF INTERNAL MAGNETIC STRUCTURE ON THE FISHBONE INSTABILITY

BY

D.W. ROBERTS, R. KAITA, F. LEVINTON, ET AL

January 1992

PRINCETON
PLASMA PHYSICS
LABORATORY

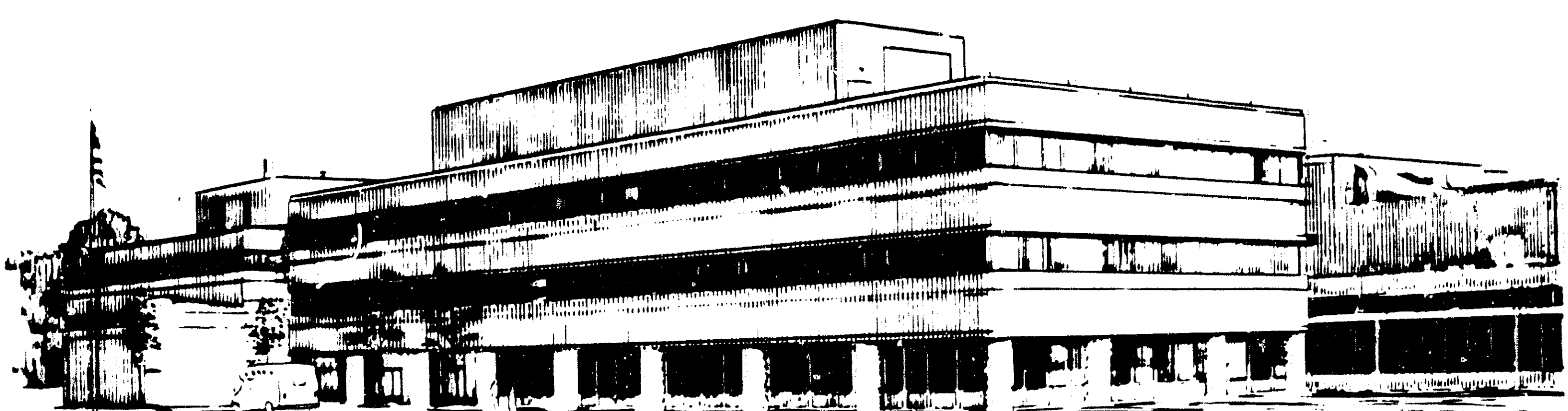

PPPL--2815

DE92 006650

The effect of internal magnetic structure on the fishbone instability

D. W. Roberts[a], R. Kaita, F. Levinton[b], N. Asakura[c], R. Bell, M. Chance, P. Duperrex[d], G. Gammel[e], R. Hatcher, A. Holland, S. Kaye, C. Kessel, H. Kugel, B. LeBlanc, J. Manickam, M. Okabayashi, S. Paul, N. Pomphrey, E. Powell[a], N. Sauthoff, S. Sesnic, H. Takahashi, R. White

Princeton University Plasma Physics Laboratory, Princeton, N.J.

Abstract

Plasmas exhibiting the "fishbone" instability studied on the PBX-M tokamak show a distinct relationship between the plasma shape, the internal magnetic structure, and the presence or absence of fast ion losses normally associated with the fishbone mode. We have, for the first time, carried out measurements of the magnetic safety factor profile in fishbone-unstable plasmas, and used the knowledge of the associated experimental equilibria to compare the stability and fast ion loss properties of these plasmas with experimental observations.

The use of auxiliary heating to achieve high temperatures in tokamak plasmas has led to the observation of a class of instabilities not fully described by simple magnetohydrodynamic (MHD) fluid theory,[1] where kinetic effects associated with the high energy particles in the plasma play an essential role. One such instability is the "fishbone" mode, which was first observed on the PDX tokamak[2] during high power, near-perpendicular neutral beam injection (NBI). The large–amplitude MHD fluctuations characteristic of the mode were associated with greatly enhanced losses of the energetic beam ions near the NBI energy, degrading the efficiency of plasma heating and limiting the attainable β $(= \frac{\langle p \rangle}{B^2/8\pi})$ values.[3] The MHD activity indicated that the poloidal and toroidal mode structure of the instability is $m/n = 1/1$ in the plasma core, with a spectrum of modes with $m \geq 2$ nearer the plasma edge. The modes rotate toroidally at approximately the precession rate of the trapped beam ions.

Fishbones have been attributed to a resonance between a population of high energy, toroidally precessing ions and an unstable (or marginally stable) internal kink mode,[4–7] or alternatively, a coupling of the hot ions, through viscous damping in the bulk plasma, to an MHD mode at the ion diamagnetic drift frequency of the thermal ions.[8] The relatively cold background plasma is described by an MHD model. The stability analysis is done via the energy principle.[1] The procedure is to add to the contribution of δW_{MHD} from the background plasma terms due to the kinetic, δW_k, and inertial, δ_I, terms, leading to a variational dispersion relation,[7]

$$D(\xi) = \delta W_{MHD} + \delta W_k + \delta_I = 0. \tag{1}$$

In this dispersion relation, the inertial term resolves the singularity in the displacement $\xi(\mathbf{r})$ at the $q(r_s) = m/n = 1$ rational surface, and its contribution is important only in this vicinity. The kinetic term arises from the hot trapped particle population. The size of this population is characterized by the hot particle beta, β_h. For even modest values of β_h ($\sim 10^{-3}$), the δW_k term can destabilize a marginally stable internal kink mode ($\delta W_{MHD} \gtrsim 0$). The resulting mode has a frequency $\omega \sim \omega_d$, where ω_d is the toroidal precession frequency of the hot trapped particles, $\omega_d \sim E_{inj} q/mrR\Omega$. Such a mode is observed experimentally.[9]

The onset conditions for the fishbone mode have been calculated for a slowing-down distribution of hot particles produced by NBI.[7] The threshold condition corresponding to the fishbone modes observed on PDX, PBX, and PBX-M is found to be

$$\beta_{crit,h} = \frac{\langle \omega_d \rangle}{\pi \omega_A}, \qquad (2)$$

where

$$\omega_A = \frac{v_A}{\sqrt{3} R r_s q'} \qquad (3)$$

is the shear Alfvén frequency evaluated at $q(r_s) = 1$, and $r_s q'$ is the magnetic shear at the rational surface.[10]

Part of the dependence of the instability on the safety factor q can be seen clearly from the expressions for $\langle \omega_d \rangle$, ω_A, and $\beta_{crit,h}$. In addition, the mode structure depends on the radial location of the rational surfaces; a measurement of $q(r)$ would provide important confirmation of the mode/hot-ion resonance model. To date, such measurements have not been made routinely and have never been made in plasmas exhibiting fishbones. Using the neutral probe beam q profile diagnostic available on PBX-M, we have obtained the necessary information to compute a plasma equilibrium that accurately models the experiment. We can use this to determine the plasma's stability, and study the predicted dependence of mode/hot–ion resonances such as those associated with the fishbone instability. This paper describes experiments in which the fishbone mode was excited and measured on PBX-M and q profile and fast ion measurements were made. These experiments provide the first comparison between the theoretically predicted dependence of the mode on the internal magnetic structure of the plasma and actual experimental measurements of $q(r)$ made by using motional Stark effect polarimetry.[11]

The fishbone experiments were conducted in low field, low current, bean-shaped plasmas. At 400 ms into the discharge, the plasma shape relaxed from a bean-shaped condition, with elongated internal flux surfaces, to a more D-shaped condition, with relatively circular internal surfaces. At the time of the relaxation, the amplitude of the fast ion losses—as seen by a perpendicularly viewing, multichannel, charge exchange analyzer (FIDE)[12]—increased sharply. Figure 1 shows the Mirnov loop signal from a coil on the outboard midplane and the fast ion signal seen by the FIDE analyzer near the NBI energy for the earlier bean-shaped, fast ion loss-free phase. Coherent fishbone oscillations are clearly seen on the Mirnov trace, but we see no evidence of fast ion losses associated with these fishbones.

Figure 2, similar to Fig. 1, shows the signal from the midplane Mirnov loop and the perpendicular fast ion losses seen by the FIDE analyzer during the later D-shaped, fast ion loss phase. As in the early, fast ion loss-free phase, coherent fishbone oscillations are clearly seen on the Mirnov trace. However, there are now also coherent bursts of fast ion losses associated with the fishbones. The similarity in the Mirnov data and in the basic plasma conditions (low density, high-β, high-β_p) indicates that during both the early and late phases, conditions are such that an MHD fishbone mode is destabilized; however, differences in the plasma equilibrium have developed during the relaxation at $t = 400$ ms causing the observed change in the fast ion loss behavior.

To determine the $q(r)$ profile during each phase, two magnetic field pitch angle (γ_p) measurements were made with the motional Stark effect (MSE) polarimeter.[13] The $q(\psi)$ and $q(r)$ profiles obtained from the γ_p data[14] for the early (fast ion loss–free) phase and the late phase are shown in Fig. 3. Comparing these results, we begin to see the changes in the equilibrium that we believe are responsible for the differences in the observed fast ion losses. At the late time, the $q(r)$ [and $q(\psi)$] profile becomes broader. In particular, the radius of the $q = 1$ surface increases. The $q(\psi)$ profile shows this more clearly, since the motion of the magnetic axis R_0 is suppressed by the use of the flux ψ as the independent variable.

During the course of our studies, several plasma discharges were observed that showed considerably enhanced fast ion losses during the late phase of the discharge. The strength of these losses increased by roughly a factor of five over the previously described losses. The Mirnov data suggest that, for these enhanced loss cases, a similar mode/hot-ion resonance is present in the core, but again the details of the equilibrium determine the degree of fast ions losses. To understand this, the MSE $\gamma_p(r)$ data were used in an equilibrium reconstruction for one of the enhanced loss shots. The $q(\psi)$ and $q(r)$ profiles for the enhanced loss case are substantially broader and more U-shaped than in the conventional late case. This observation is consistent with the difference in the q profile between the conventional, fast ion loss-free early phase and the fast ion loss late phase. The observations indicate that the q profile broadens and flattens, and as the radius of the $q = 1$ surface increases, the strength of the fast ion losses associated with the fishbones rises accordingly.

We compared these results with the fast ion losses predicted by the White–Chen fishbone model by using the guiding center code ORBIT, developed by White and Chance.[15] The code studies the fast ion losses resulting from a perturbation of the axisymmetric equilibrium magnetic field due to the MHD modes of the mode/hot–ion resonance. Previous fast ion loss studies employing ORBIT have used analytic equilibria, or numerical equilibria in which one or more of the quantities $p(\psi)$, $q(\psi)$, or $g(\psi)$ had an assumed analytic form.[4,15] With the magnetic pitch angle data from our fishbone experiments and the resulting equilibrium reconstructions they provide, we have for the first time compared the predictions of the White–Chen model for fast ion losses with the observed losses and accurate equilibrium information in each of our experimental conditions.

The fast ion loss calculations made by using ORBIT require the equilibrium information discussed above as well as amplitudes of each poloidal and toroidal (m, n) component of the MHD activity. To obtain the amplitudes of each (m,n) component, we incorporated both our measured Mirnov data and stability results from the PEST ideal MHD stability code.[16] Using PEST, we found that the fast ion loss-free phase of the shaped, fishboning plasmas was unstable to the internal kink. From this analysis, we determined the maximum amplitude of each (m,n) mode measured at the plasma edge. For the late, fast ion loss phase of the shaped, fishboning plasmas, we carried out stability analyses for both the conventional and enhanced loss cases. The PEST results for each case indicate that the plasmas were unstable to the internal kink as in the earlier time. The broad, flat q profile in the later cases, however, leads to a significantly larger radial extent for the internal kink activity.

The predominant MHD modes found by using PEST and our Mirnov measurements for the early and late phases were quite similar: the basic character of the MHD activity seen in the Mirnov data was essentially unchanged by the shape relaxation at $t = 400$ ms, the mode analysis of the Mirnov data showed that the predominant (m,n) contributions to the MHD activity at the early and late times were $m = 1$, $n = 1$ and $m = 2$, $n = 1$, and the frequencies at the early and late times differed only slightly. However, the fast ion behavior for each phase was quite different. These results indicate that the basic fluid stability conditions for driving fishbones exist in the core at both the early and late times.

Because the fluid stability for both the fast ion loss-free phase and the fast ion loss phase were the same, we next examined the kinetic stability properties of each time, using the kinetic dispersion relation solver CHEN,[7] developed by White and Chen and modified for this work to allow more accurate reconstruction of the experimentally determined q profile. Each of our cases was found to be unstable to the fishbone mode according to these calculations. The differences in measured fast ion losses are thus due neither to gross differences in MHD behavior nor in kinetic stability. Rather, the relationship between the internal profiles and the fast ion drifts associated with the mode must explain the difference in behavior.

To verify this relationship, we used our experimental equilibria, the measured neutral beam parameters, and the MHD mode amplitudes described above to obtain the calculated fast ion losses with the ORBIT code. Table I summarizes the observed and calculated mode properties for the fishbone observations in each of our three cases. The fraction of beam particles that are trapped is obtained from the ORBIT calculation. The shear Alfvén frequency, ω_A, is found using Eq. (3) and the equilibrium results for each case. The average precession rate for the trapped particles, $\langle\omega_d\rangle$, is obtained from ORBIT. The critical hot particle β, $\beta_{crit,h}$, is given by Eq. (2), using the values for $\langle\omega_d\rangle$ and ω_A discussed above. Finally, the mode frequency is equal to $\langle\omega_d\rangle/2\pi$. The observed and calculated mode frequencies are in agreement. Note that the fishbone threshold suggests that the early, fast ion loss-free case is at least as unstable as the later times. The fraction of fast ions trapped within the kink resonance at $q = 1$ seems to confirm the relationship between q profile shape and observed losses.

The results of our ORBIT calculations for the fast ion losses predicted for each of our cases are shown in Figure 4. The plots show the energy distribution of exiting particles for the early, late, and enhanced loss cases. From the figure, we see that the magnitude of fast ion losses in the conventional late case is about seven times greater than in the early case. This agrees with our experimental observations, where in the early case, we could discern no fast ion losses above the noise. The magnitude of the fast ion losses for the enhanced loss case shows an increase of two to three over the conventional late case. Comparing the relative amplitude of the losses for the conventional and enhanced loss cases, we find that our results obtained from the White–Chen model substantially agree with the experimentally observed variation in fast ion losses.

We have observed that in plasmas exhibiting the fishbone instability, the details of the equilibria—related in our case to the plasma shape and q profile—can greatly affect the observed fast ion losses. While our results suggest that plasmas of different shapes may not differ in their stability against fishbone modes, the influence of shape on the details of the equilibrium profiles can affect the fast ion losses associated with these fishbones. This can have important implications in the operation of a burning plasma experiment or a fusion test reactor, in which the loss of high energy particles, either from auxiliary heating or from fusion products themselves, could greatly affect the performance of the device.[17]

This work was supported by U.S.DOE Contracts No. DE-AC02-76-CH03073 and DE-AC03-86-ER80409. One of the authors (D.R.) has been under appointment to the Magnetic Fusion Science Fellowship program administered by Oak Ridge Associated Uni-

versities for the U.S. Department of Energy.

[(a)] University of California, Lawrence Livermore National Laboratory, Livermore, CA.

[(b)] Fusion Physics and Technology, Torrance, CA.

[(c)] University of Tokyo, Tokyo, Japan.

[(d)] Ecole polytechnique fédérale de Lausanne, Lausanne, Switzerland.

[(e)] Grumman Aerospace Corporation, Bethpage, NY.

Figures

FIG. 1. The midplane Mirnov coil and perpendicular fast ion (FI) loss data for the fast ion loss-free phase of the shaped, fishboning plasma case.

FIG. 2. The midplane Mirnov and FI loss data for the late, fast ion loss phase of the shaped, fishboning plasma case. The figure shows a series of fishbone oscillations, including the coherent fast ion losses that appear at the late time.

FIG. 3. A comparison between the $q(\psi)$ and $q(r)$ profiles for the early and late phases of the shaped, fishboning plasmas.

FIG. 4. The energy distribution of the predicted fast ion losses for each of our shaped, fishboning plasma cases. The magnitude of the losses for each case are in good agreement with the experimental observations.

Tables

TABLE I. A summary of the observed and calculated fishbone properties for each phase of our shaped, fishboning plasmas.

References

[1]J. P. Freidberg, *Ideal Magnetohydrodynamics*, Plenum Press, New York, 1987.

[2]K. McGuire *et al.*, Phys. Rev. Lett. **50**, 891 (1983).

[3]D. Johnson *et al.*, in *Plasma Physiscs and Controlled Nuclear Fusion Research 1982*, (Proc. of the 9th Internat. Conf., Baltimore, 1982), Vol. 1, pp. 9–26, Vienna, 1983, IAEA.

[4]R. B. White *et al.*, Phys. Fluids **26**, 2958 (1983).

[5]L. Chen, R. B. White, and M. N. Rosenbluth, Phys. Rev. Lett. **52**, 1122 (1984).

[6]L. Chen *et al.*, in *Plasma Physcis and Controlled Nuclear Fusion Research 1984*, (Proc. of the 10th Internat. Conf., London, 1984), Vol. 2, pp. 59–67, Vienna, 1985, IAEA.

[7]R. B. White, L. Chen, R. Romanelli, and R. Hay, Phys. Fluids **28**, 278 (1985).

[8]B. Coppi and F. Porcelli, Phys. Rev. Lett. **57**, 2272 (1986).

[9]R. Kaita *et al.*, Phys. Fluids B **2**, 1584 (1990).

[10]R. B. White, M. N. Bussac, and F. Romanelli, Phys. Rev. Lett. **62**, 539 (1989).

[11]F. M. Levinton *et al.*, Phys. Rev. Lett. **63**, 2060 (1989).

[12]R. Kaita, R. J. Goldston, D. Meyerhofer, and J. Eridon, Rev. Sci. Instrum. **52**, 1795 (1981).

[13]F. M. Levinton, G. M. Gammel, R. Kaita, H. W. Kugel, and D. W. Roberts, Rev. Sci. Instrum. **61**, 2914 (1990).

[14]D. W. Roberts, R. Kaita, and F. M. Levinton, Rev. Sci. Instrum. **61**, 2932 (1990).

[15]R. B. White and M. S. Chance, Phys. Fluids **27**, 2455 (1984).

[16]R. C. Grimm, J. M. Greene, and J. L. Johnson, in *Methods in Computational Physics,* Vol. 16, pp. 253–280, Academic Press, New York, 1976.

[17]H. P. Furth, R. J. Goldston, S. J. Zweben, and D. J. Sigmar, Nucl. Fusion **30**, 1799 (1990).

Mode characteristics	Early	Late	Enhanced Loss
Observed mode frequency (kHz)	15 – 25	10 – 20	10 – 20
Fraction of beam trapped (%)	64	82	79
Fraction of beam trapped, $q < 1$ (%)	8	21	42
Shear Alfvén, ω_A(sec^{-1})	3.8×10^6	2.6×10^6	1.8×10^6
Precession rate $\langle \omega_d \rangle$(sec^{-1})	8.8×10^4	9.3×10^4	1.0×10^5
Fishbone threshold, $\beta_{h,crit}$	7.4×10^{-3}	1.1×10^{-2}	1.8×10^{-2}
Calculated mode frequency (kHz)	14	15	16

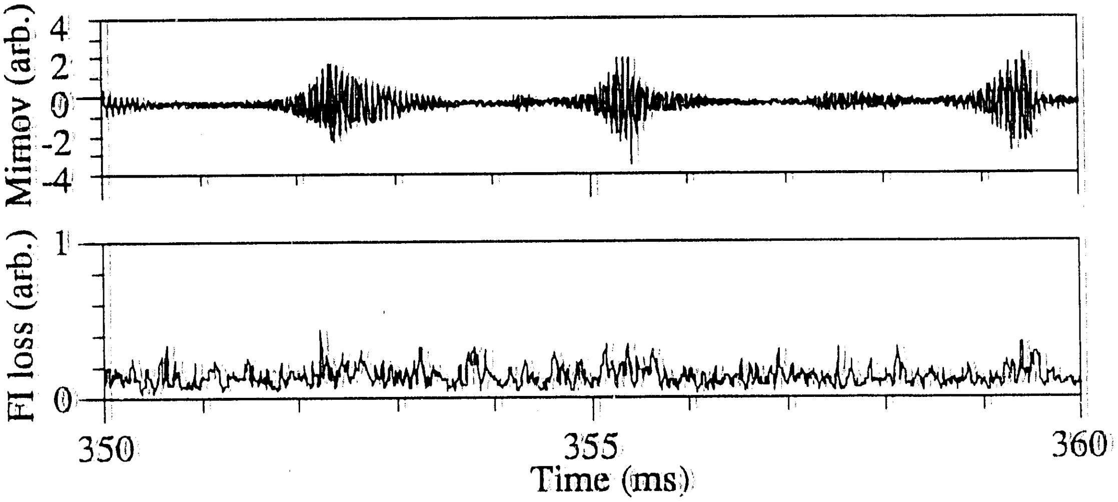

Figure 1.

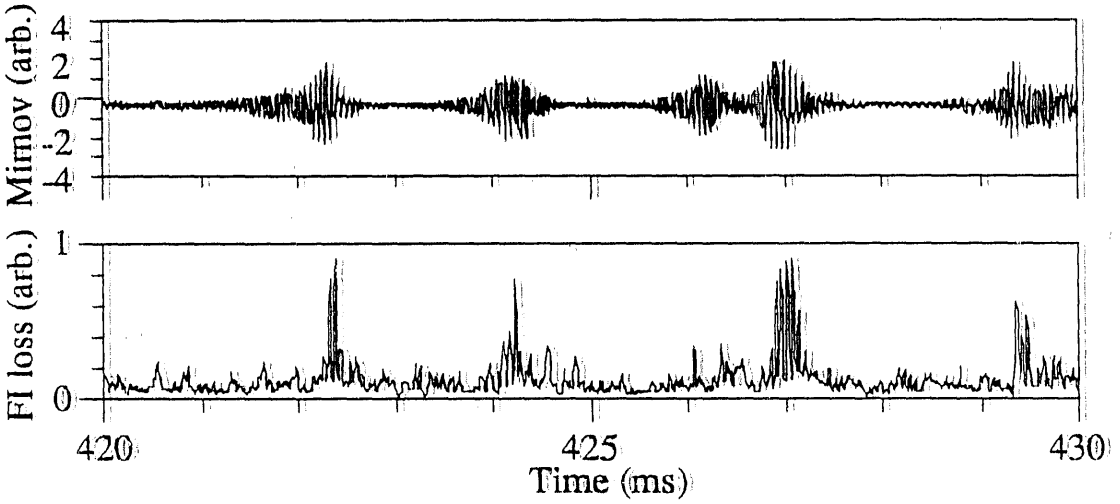

Figure 2.

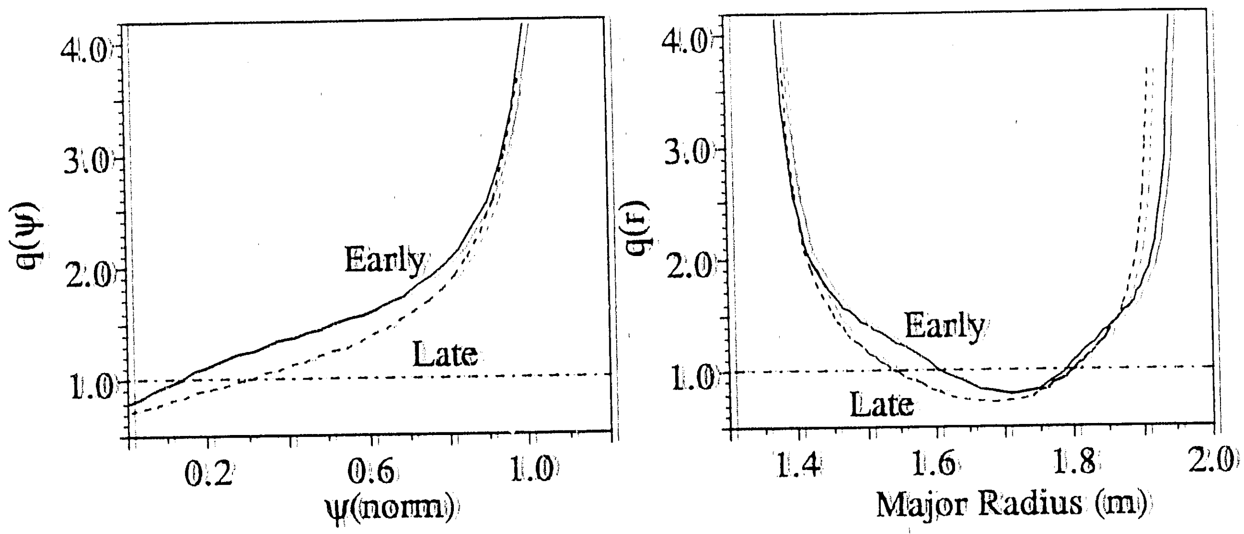
4.0
3.0
2.0
1.0
q(ψ)
Early
Late
0.2
0.6
1.0
ψ(norm)
4.0
3.0
2.0
1.0
q(r)
Early
Late
1.4
1.6
1.8
2.0
Major Radius (m)

Figure 3.

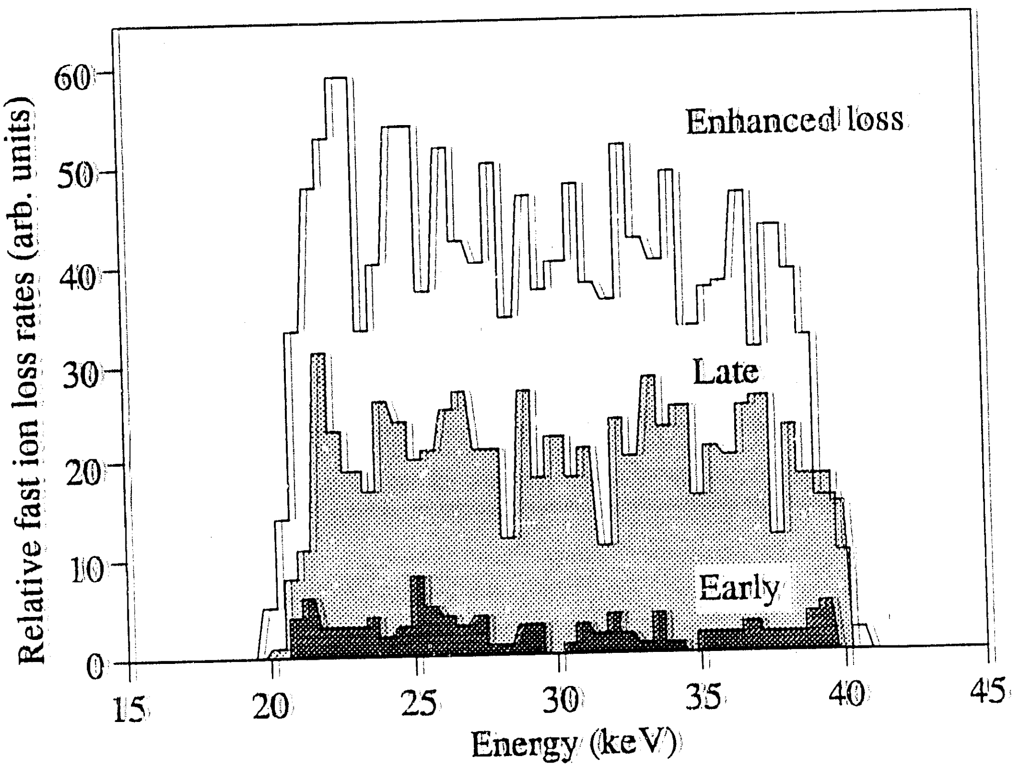
Relative fast ion loss rates (arb. units)
60
50
40
30
20
10
0
Enhanced loss
Late
Early
15
20
25
30
35
40
45
Energy (keV)

Figure 4.

EXTERNAL DISTRIBUTION IN ADDITION TO UC-420

Dr. F. Paoloni, Univ. of Wollongong, AUSTRALIA
Prof. M.H. Brennan, Univ. of Sydney, AUSTRALIA
Plasma Research Lab., Australian Nat. Univ., AUSTRALIA
Prof. I.R. Jones, Flinders Univ, AUSTRALIA
Prof. F. Cap, Inst. for Theoretical Physics, AUSTRIA
Prof. M. Heindler, Institut für Theoretische Physik, AUSTRIA
Prof. M. Goossens, Astronomisch Instituut, BELGIUM
Ecole Royale Militaire, Lab. de Phy. Plasmas, BELGIUM
Commission-European, DG. XII-Fusion Prog., BELGIUM
Prof. R. Boucique, Rijksuniversiteit Gent, BELGIUM
Dr. P.H. Sakanaka, Instituto Fisica, BRAZIL
Instituto Nacional De Pesquisas Espaciais-INPE, BRAZIL
Documents Office, Atomic Energy of Canada Ltd., CANADA
Dr. M.P. Bachynski, MPB Technologies, Inc., CANADA
Dr. H.M. Skarsgard, Univ. of Saskatchewan, CANADA
Prof. J. Teichmann, Univ. of Montreal, CANADA
Prof. S.R. Sreenivasan, Univ. of Calgary, CANADA
Prof. T.W. Johnston, INRS-Energie, CANADA
Dr. R. Bolton, Centre canadien de fusion magnétique, CANADA
Dr. C.R. James,, Univ. of Alberta, CANADA
Dr. P. Lukác, Komenského Universzita, CZECHO-SLOVAKIA
The Librarian, Culham Laboratory, ENGLAND
Library, R61, Rutherford Appleton Laboratory, ENGLAND
Mrs. S.A. Hutchinson, JET Library, ENGLAND
Dr. S.C. Sharma, Univ. of South Pacific, FIJI ISLANDS
P. Mähönen, Univ. of Helsinki, FINLAND
Prof. M.N. Bussac, Ecole Polytechnique,, FRANCE
C. Mouttet, Lab. de Physique des Milieux Ionisés, FRANCE
J. Radet, CEN/CADARACHE - Bat 506, FRANCE
Prof. E. Economou, Univ. of Crete, GREECE
Ms. C. Rinni, Univ. of Ioannina, GREECE
Dr. T. Mual, Academy Bibliographic Ser., HONG KONG
Preprint Library, Hungarian Academy of Sci., HUNGARY
Dr. B. DasGupta, Saha Inst. of Nuclear Physics, INDIA
Dr. P. Kaw, Inst. for Plasma Research, INDIA
Dr. P. Rosenau, Israel Inst. of Technology, ISRAEL
Librarian, International Center for Theo Physics, ITALY
Miss C. De Palo, Associazione EURATOM-ENEA , ITALY
Dr. G. Grosso, Istituto di Fisica del Plasma, ITALY
Prof. G. Rostangni, Istituto Gas Ionizzati Del Cnr, ITALY
Dr. H. Yamato, Toshiba Res & Devel Center, JAPAN
Prof. I. Kawakami, Hiroshima Univ., JAPAN
Prof. K. Nishikawa, Hiroshima Univ., JAPAN
Director, Japan Atomic Energy Research Inst., JAPAN
Prof. S. Itoh, Kyushu Univ., JAPAN
Research Info. Ctr., National Instit. for Fusion Science, JAPAN
Prof. S. Tanaka, Kyoto Univ., JAPAN
Library, Kyoto Univ., JAPAN
Prof. N. Inoue, Univ. of Tokyo, JAPAN
Secretary, Plasma Section, Electrotechnical Lab., JAPAN
S. Mori, Technical Advisor, JAERI, JAPAN
Dr. O. Mitarai, Kumamoto Inst. of Technology, JAPAN
J. Hyeon-Sook, Korea Atomic Energy Research Inst., KOREA
D.I. Choi, The Korea Adv. Inst. of Sci. & Tech., KOREA
Prof. B.S. Liley, Univ. of Waikato, NEW ZEALAND
Inst of Physics, Chinese Acad Sci PEOPLE'S REP. OF CHINA
Library, Inst. of Plasma Physics, PEOPLE'S REP. OF CHINA
Tsinghua Univ. Library, PEOPLE'S REPUBLIC OF CHINA
Z. Li, S.W. Inst Physics, PEOPLE'S REPUBLIC OF CHINA
Prof. J.A.C. Cabral, Instituto Superior Tecnico, PORTUGAL
Dr. O. Petrus, AL I CUZA Univ., ROMANIA
Dr. J. de Villiers, Fusion Studies, AEC, S. AFRICA
Prof. M.A. Hellberg, Univ. of Natal, S. AFRICA
Prof. D.E. Kim, Pohang Inst. of Sci. & Tech., SO. KOREA
Prof. C.I.E.M.A.T, Fusion Division Library, SPAIN
Dr. L. Stenflo, Univ. of UMEA, SWEDEN
Library, Royal Inst. of Technology, SWEDEN
Prof. H. Wilhelmson, Chalmers Univ. of Tech., SWEDEN
Centre Phys. Des Plasmas, Ecole Polytech, SWITZERLAND
Bibliotheek, Inst. Voor Plasma-Fysica, THE NETHERLANDS
Asst. Prof. Dr. S. Cakir, Middle East Tech. Univ., TURKEY
Dr. V.A. Glukhikh, Sci. Res. Inst. Electrophys. I Apparatus, USSR
Dr. D.D. Ryutov, Siberian Branch of Academy of Sci., USSR
Dr. G.A. Eliseev, I.V. Kurchatov Inst., USSR
Librarian, The Ukr. SSR Academy of Sciences, USSR
Dr. L.M. Kovrizhnykh, Inst. of General Physics, USSR
Kernforschungsanlage GmbH, Zentralbibliothek, W. GERMANY
Bibliothek, Inst. Für Plasmaforschung, W. GERMANY
Prof. K. Schindler, Ruhr-Universität Bochum, W. GERMANY
Dr. F. Wagner, (ASDEX), Max-Planck-Institut, W. GERMANY
Librarian, Max-Planck-Institut, W. GERMANY
Prof. R.K. Janev, Inst. of Physics, YUGOSLAVIA

END

DATE FILMED

3 / 3 / 92